CrystEngComm

Accepted Manuscript

ROYAL SOCIETY OF CHEMISTRY

www.rsc.org/crystengcomm

A Heterometallic Nano Sized Tube $\{Fe[(CN)_6]_2[Co(LN_3O_2)]_3\}n$ and Two of Its Lamellar Polymorphous Isomers†

F. Pan,*[ab] S. Gao*[a] and H. Z. Liu*[b]

Received 00th January 20xx,

Accepted 00th January 20xx

DOI: 10.1039/x0xx00000x

www.rsc.org/

Single crystals of three polymorphous compounds were synthesized started from two building blocks $[Fe(CN)_6]^{3-}$ and $[Co(L_{N3O2})]^{2+}$ (L is a Schiff-base macrocyclic ligand derived from the condensation of 2,6-diacetylpyridine with 3,6-dioxaoctane-1,8-diamine) using a crystallization condition control. They are all consisting of electroneutral skeletons made up of Fe_6Co_6 twelve-metal ring units, which is the smallest enclosed circle in these structures: 1 is comprised of 1 D nanometer-diameter tubes possessing nanometer sized tunnels (0.58 nm × 0.74 nm); 2 and 3 are based on piling up 2D lamellar layers in (6, 3) and (4, 4) network respectively. Magnetic studies indicate ferromagnetic interaction between cyanide bridged cobalt (II) and iron (III) in each compound.

Owing to the advances in computer processing technology and more efficient X-ray diffraction devices, crystal design and engineering as the basis of modern solid material science developed rapidly in the last twenty years[1]. As a result, a number of crystals with interesting architectures and corresponding properties have been reported and some of their syntheses have been well reviewed and generalized, in spite of that, it is still a great challenge predicting the atomic arrangements and structural dimensionalities in new compounds because of the complicated factors in the crystal formation processes: e.g. solvent system, coordination tendency of organic ligands, metal to ligand ratio, templates and the counter-anions, *etc*[2]. A promising approach for controlling the formation of the molecules is to assemble two building blocks that usually are transition metal complexes, one with terminal ligands acting as bridges and another one with available coordination sites. $[M(CN)_n]^{m-}$ (M = Cr^{III}, Mn^{III}, Fe^{III}, Fe^{II}) complexes are very popular building blocks, the resulting molecular assemblies often show characteristic multidimensional architectures exhibiting para-, ferro-, ferri- or meta-magnetism[3, 4], furthermore, many researchers in the area of molecule magnetism also focused upon synthesizing structures of low dimensionality in purpose of getting large spin ground states preferentially combined with magnetic anisotropy[5, 6]. In further syntheses, these $[M(CN)_n]^{m-}$ precursors are combined with complexes such as $[M^{II}(L)]^{m+}$ (M^{II} = Mn, Ni, Co, Cu, and L = diamine or polyamine or Schiff-base), which has led to a variety of architectures in cyanide family[4-6, 7]. The trying of macrocycles as ligand L resulted in considerable interests in the investigations of metal ion recognition in supramolecular coordination chemistry for the presence of a central cavity[8], a classic equatorial in-plane 15-membered pentadentate macrocycle L_{N3O2} (Scheme **1**) with N_3O_2 donor atoms, synthesized and characterized by Nelson and his coworkers[9], was used in this work, several structures of these specific metal-macrocylic ligand complexes: $[Mn^{II}L_{N3O2}(NCS)_2]$, $[Mg^{II}L_{N3O2}(H_2O)_2]$, $[Fe^{II}L_{N3O2}(CN)_2]$ have been reported and used for building the extended structures with $[M^{III}(CN)_6]^{3-}$ or $[M^{II}(CN)_6]^{4-}$ units[7, 9, 10].

Structural dimensionality is a crucial factor defining properties of solid materials, nevertheless, with coordination chemistry methods, not only specific dimensionality could be well controlled in series[4, 6, 11], but also the structural dimensionalities change under the follow-up operations. In the recent work of Wu et al., a "rolling up" synthetic strategy for sheet/tube superstructure transformation was achieved[12], by tuning the interaction in between asymmetric layers with different amine templates, the 2D sheets transform to 1D Metal Organic NanoTube (MONT) structure, immediately after that, some other example has been reported with similar strategy[13]. Inspired but different from those upfront works, we synthesized and studied a series of heterometallic coordination isomers based on the precursors of $[Co(L_{N3O2})]^{2+}$ and $[Fe(CN)_6]^{3-}$ including a MONT one. The pentagonal bipyramidal precursor $[Co(L_{N3O2})]$ was synthesized by a Schiffbase condensation of 2,6-diacetylpyridine and 3,6-dioxaoctane -1,8-diamine (shown in Scheme 1) in the presence of Co^{II} salt as a template, then reacted with $[Fe(CN)_6]^{3-}$, three extended structures **1**, **2** and **3** were built. To get the pure structure-independent samples for further property characterizations, a reacting dynamics control during crystals'

[a] *Beijing National Laboratory for Molecular Sciences, State Key Lab of Rare Earth Materials Chemistry and Applications, College of Chemistry and Molecular Engineering, Peking University, Beijing 100871, P. R. China.* gaosong@pku.edu.cn

[b] *Key Laboratory of Green Process and Engineering, State Key Laboratory of Biochemical Engineering, Institute of Process Engineering, Chinese Academy of Sciences, Beijing 100190, PR China.* pfeng@ipe.ac.cn *and* hzliu@ipe.ac.cn

† Electronic Supplementary Information (ESI) available: experimental details, PXRD patterns, CIF files, more structural diagrams, selected bond lengths and angles and more discussion and figures of magnetic data. CCDC: 1056047, 1056035 and 1056048. For ESI and crystallographic data in CIF or other electronic format see DOI: 10.1039/x0xx00000x

formatting was tried, feeding ratio and the diffusion rate were considered and some rough rules were observed that Large Co/Fe concentration ratio (Co/Fe = 10) under slow diffusion (reactants in two arms of H tube) tends to form compound **1**, whose structure is made up of one dimensional nanometer sized tubes and possessing 1 D tunnel, the section of tunnel is rhombic shaped with the diagonals estimated 0.58 and 0.74 nanometer (Figure S4a); Diffusing slowly using a H tube but with relatively low metal concentration ratio (Co/Fe = 1.5) tends to form **3** which is a 2D lamellar compound with rectangle latticed planes; A relative fast diffusion that layering reactant solutions with higher concentration in a test tube resulted in another 2D lamellar structure of compound **2** possessing the brick-wall latticed network, all the experimental details are provided in supplementary materials.

From the structural perspective, in common, these three compounds are all made up of $[Fe(CN)_6]^{3-}$ and $[Co(L_{N3O2})]^{2+}$ as building blocks, written as $\{Fe[(CN)_6]_2[Co(L_{N3O2})]_3\}_n$ in absence of solvent molecules, the metal ratio (Fe/Co = 2/3) ensures electronically neutral frameworks in each one. A twelve-member rings consisting of six iron blocks and six cobalt blocks alternately as shown in Figure S2 were observed in each structure, the ring is the basic unit for their respective further extended structures. In each structure hepta-coordinated cobalt ions provide two ***trans*** coordinating sites combining to two iron units through cyanides, so all the cobalt units are only acting as in-ring-connectors, extended constructions are built by extra CN^- ligands in $[Fe(CN)_6]^{3-}$. Detailed crystallographic data are summarized in Table S3, and the key bond lengths and angles are listed in Table S6. Detailed molecular geometries were retrieved from the cif files.

There are six types of structurally independent cobalt ions in the tubular structure of **1**, they are all situated in a distorted pentagonal bipyramid environment: three N atoms and two O atoms in one L_{N3O2} constitute the equatorial of the bipyramid, two N atoms from two $[Fe(CN)_6]^{3-}$ blocks are situated at the two vertexes in opposite sides. The Co–N bond lengths along the axe direction with N atoms donated by cyanides are ranging from 2.076 Å to 2.183 Å, those are approximate to the Co–N bond lengths (2.073 Å–2.220 Å) in the equatorial plane with pyridines' N atoms but relatively shorter than the Co–O bonds (2.250 Å–2.299 Å) in the equatorial plane. So the cobalt is situated in a slightly squashed pentagonal bipyramid. There are four types of structurally independent iron ions, the variation of cyanide concerned bond parameters are quite limited: Fe–C bond length varies from 1.885 Å to 1.962 Å, the range of Fe–C–N angle is 175.3°–179.1° affording quite linear connections in contrast to the Co–N–C angles (148.2°–166.9°).

In order to emphasize the tubular skeleton some L_{N3O2} ligands are dimmed in Figure 1a, it demonstrates that the tube is a semi-enclosed architecture formed by curling the cyanide bridged Fe–Co network extending along ***a*** axe direction. The diameter of the cylindrical metal framework was measured to be 1.2 nm (Figure S4b) which is large in so called metal organic nanotubes (MONTs) series[12-14]. All the pyridine ring of the L_{N3O2} ligands pointing outward from the tube wall, these out-stretching aromatic groups lead to a steric hindrance effect that weaken the inter-tube interactions from neighbors, which is consistent with its non-long-range magnetic behaviors. Figure 1b is a connection schematic diagram in which orange and purple balls are representing iron and cobalt atoms respectively and the gray sticks are standing for connections through cyanides, it shows that the cobalt ions are of only one connection pattern that is connecting two irons at their axe coordinating sites, and there are three connection types of iron atoms: **Fe1** and **Fe2** are providing three cyanides for further connection (*via* Co to next Fe) in *mer*– pattern, which makes these iron ions triple connecting nodes; **Fe3** provides four connecting cyanides being a tetra connecting node; As for **Fe4**, two *trans* cyanide are provided for further connecting, it is not functionalized as a node. In topology point of view, the structural lattice is constructed by pentagons as highlighted by the red lines in this figure, so the surface is a pronounced Archimedean plane, namely the plane is made of only one type of polygon, start from a node, the connection number is equal to 3 or 4, so the skeleton of **1** is made up of a (5^3_4) topology lattice.

In the packing graph (Figure 1d) facing the tube's growing direction, we can see every tube has four neighboring tubes, they are repelling each other spatially due to their outstretched aromatic rings on the surfaces, and there is no effective π–π interaction between the adjacent tubes because of the large distance and less effective angles between the aromatic rings. The 3D structure has been formed by the Van der Waals interaction and the H-bond interaction caused by methyl or other heteroatom on the outside wall. Masses of solvent water molecules were observed filling in the gap between and inside the tubes, a rhombic-section tunnels are formed in a size of 0.58 nm × 0.74 nm (estimated by creating a dummy atom of given diameters in the Van der Waals radii piling graph as shown in Figure S4a). For further studying the relationships with the other two planar structures, the tube was redrawn as a square prism growing along ***a*** direction basing on the original metal connections in Figure 1c, each side wall is a ladder-liked network made up of repeating twelve metal rectangles, and for each rectangle, four vertexes and two midpoints on long edges are all occupied by iron ions, and every cobalt ion situates between each pair of adjacent irons. There are two types of way for the ladders' conjunctions in the tubular structure: one is that two ladders are aligning rightly like the front and bottom walls in Figure 1c; the other situation is that the ladders slip in a half edge of rectangle from each other as the way front and up walls connect in Figure 1c.

The metal-ligand combinations in the planar structures of **2** and **3** are similar to **1**: cobalt ions are situated in a

slightly squashed pentagonal bipyramid, in their equatorial plane the bond lengths of Co–N/O are 2.108 Å – 2.308 Å, Co–N bond lengths along the axe direction are 2.080 Å – 2.136 Å. The cyanide concerned bond angels Fe–C–N: 167.5°–179.5°; Co–N–C: 152.1°–167.2°. There are only one structurally independent iron ion and two types of cobalt ions in compound **2**, which is partly because some atoms are located at high symmetric position crystallographically: **Co1** and the *para* C7 and N7 atoms of pyridine ring are situated on the two fold symmetric axe, as shown in Figure 2a, the Fe_6Co_6 twelve metal rings with chair conformation form a kind of (6, 3) planar network, every iron ion connects to three other iron blocks *via* cyanides and cobalt blocks. The network can be also considered as ladders spreading along ***a–b*** direction with an interlaced conjunction pattern mentioned above. Seeing the packing picture of **2** along ***b*** axe in Figure 2b, there is barely approach for adjacent layers' interaction through aromatic rings, the solvent molecules are filling in between the layers or in the gaps of Fe and Co fragments. **2** loses its solvents very easily under room temperature and atmospheric pressure, the X-ray diffraction was operated at a low temperature as 198 K.

In **3**'s structures (Figure 2c), there are two types of iron ions in different combining patterns, **Fe1** situates at the vertex of a rectangle shared by four rectangles, **Fe2** situates at the midpoint of a long edge shared by two rectangles. Like the former two compounds, the plane can also be considered as ladders along ***c*** direction, and the ladders are aligning rightly which is also one way in constructing the tubular architecture of compound **1**. The packing of compound **3** is shown in Figure 2d, the planes are spreading along ***ac*** plane, viewing along ***a*** direction, the ABAB typed piling of wavy layers could be observed, the lamellae are layering alternatively: one is up the next is down along ***b*** direction. In accordance with Figure 3d, the top two layers are piling closer, because the ridgy parts in one layer just embed in the sunken parts of the other layer, on the contrary, the second and third layers are meeting at their apophyses which results in large gaps between them. A large proportion of solvent molecules are situating between 2n and 2n+1 layers, where it possessing the gaps, most of the solvents are close to surfaces of layers and the 1D channels are formed along ***a*** direction (Figure S3a). A Van der Waals radii filling diagram is shown in Figure S5b, were the solvent molecules removed, the tunnels' sectional area will be as large as 0.36 nm × 0.90 nm (Figure S5c); while between 2n–1 and 2n layers, the ligands from two layers are very close, so relative larger inter-plan interactions comparing with **2** is expectable, that is consistent with its magnetic properties.

In summary, structures of these three compounds are closely related owing to the existence of 1D infinite ladder substructures in each skeleton, start from which, the two plane networks of **2** and **3** can be generalized as aligning ladders in different rules: aligning rightly in compound **3** and aligning interlacely in compound **2**. If the ladders conjunct in an alternating way, the 2D network will roll up and the skeleton of compound **1** will be formed. From a synthetic point of view, in this system, a relatively fast diffusion of the two building block reactants tends to form the 2D layer with a loose symmetric piling up as **2**; slow diffusion reaction helps forming asymmetric and tunnel possessed structures of **1** and **3**. **3** may be considered as a semi-formation during a plan-to-tube rolling-up.

All these compounds have Fe–Co twelve-metal rings as the smallest enclosed circles in their respective structures, the average number of neighboring metals combined by cyanide is equal to 2.4 which is relatively low in cyanide-bridge compound series[15], so the long ranged order originated from direct cyanides bridging seems unreachable. Supported by the magnetization measurements and ab initio calculations reported, seven-coordinated Co^{II} with pentagonal bipyramid geometry exhibits very large but positive anisotropy[16, 17], however a field induced slow relaxations in Co^{II} with pentagonal bipyramid coordination was observed recently[18] owing to the direct spin-phonon process in the compounds of Kramers ions[16]. As for the series in this work only ferromagnetic interactions between Fe^{III} and Co^{II} were observed in the magnetic measurements, the anisotropy of Co^{II} is presumed to be dismissed by partially orthogonalization in the spiral connection of metals. The temperature dependence of their magnetic susceptibilities under a 1 kOe applied field is shown in Figure S9 and S10a, the experimental $\chi_m T$ values per Co_3Fe_2 at 300 K are 9.0, 8.68 and 8.79 cm^3Kmol^{-1} for **1, 2** and **3**, respectively. Presuming *g*Fe = 2.0 and a spin-only contribution was considered, got *g*Co values being equal to 2.42, 2.37 and 2.37, The relative big g is owing to the considerable contribution from the orbital angular momentum of Co^{II}. For all compounds the high-temperature data obey the Curie-Weiss law, giving Weiss temperatures are 0.39, 1.62 and 2.36 K. The positive Weiss temperature values indicate dominant ferromagnetic (FO) couplings of cyanide bridged iron and cobalt ions in each compound. Different from **1** and **2**, a relative strong inter-layer interaction is expected in **3** through its alternating closely packing. In Figure S10a, **3**'s $\chi_m T$ value is increasing slowly under the decreasing temperature, a sudden rising occurs around 20 K, and the curve gets a peak at 4.3 K then falls swiftly. The summit value 54.4 cm^3Kmol^{-1} is much larger than **1** and **2** (16.83 cm^3Kmol^{-1} for **1** and 14.34 cm^3Kmol^{-1} for **2**) indicating a possible spontaneous magnetization at this temperature. The FCM–ZFCM curve (Figure S10a) has a sharp peak at 5.0 K, which is a feature of anti-ferromagnetic ordering, and then in lower temperature the two branches deviate from each other indicating a spontaneous magnetization below 5.0 K. In the field dependent magnetization curve at 1.9 K shown in Figure S10b, the pronounced sig-mod shape indicates **3** being a meta-magnetic compound: it transfers from an anti-ferromagnetic state caused by the interlayer interaction under lower temperature and weak magnetic field to a state dominated by intra-plane Fe-Co

ferromagnetic interaction at higher field. The hysteresis at higher fields looks like a thin butterfly which is also a feature of meta-magnetism, and the accurate transition filed (Hc = 550 Oe) was obtained by differentiating the M - H curve. More magnetic measurements and further analyses of **3** are given in the supplementary information S7.

Conclusions

In this work, we synthesized an air stable Co^{II} macrocyclic precursor using cobalt ion as the template. This precursor was taken as a building block, with $[Fe(CN)_6]^{3-}$, we built three extended polymorphous structures **1**, **2** and **3** under different crystallization conditions. Their extended structures are all based on the Fe_6Co_6 twelve metals ring units, their electrically neutral skeletons are isomers to each other being written as $\{Fe[(CN)_6]_2[Co(L_{N3O2})]_3\}_n \cdot x$solvent, and their different frameworks are due to the different conjunctions of the ladder like substructures. As for their magnetic properties, only ferromagnetic interactions between cyanide bridged Fe and Co ions have been observed in measuring **1** and **2**, which is corresponding to their spiral combinations and loose alignment of tubes or layers. In **3**, asymmetry wavy layers are aligning more compactly to its neighbors alternately which create approaches for inter-layer interactions, as a result, long range ordering and week spontaneous magnetization was observed at low temperatures. A reacting dynamics control was tried in their preparations, indicating that a fast diffusion of the two building block reactants lead to the 2D layer with a loose symmetric piling up of **2**; slow diffusion reaction helps forming asymmetric and tunnel possessed structures of **1** and **3** in different concentration ratios respectively. From the "rolling up" point of view, **3** just meets the requirements[12] of transiting to tubular structure that possessing asymmetric hybrid layers of ABAB type. Indeed, **3** has already have the analogical tunnel structure of **1 (**Figure S4-5**)**, **3** could be imagined as a semi-finished structure in the process of rolling-up, the solidification of a specific period during the plane/tube evolution. With the unsolved complexities in designing molecular material, the building block strategy does not always obtain the unique predicted structure, a wide range of factors deserve putting into practice in rational preparations.

Acknowledgement

This work was supported by the State Major Basic Research Development Program of China (2013CB933401, 2013CB632602), "973"Project (2012CBA01202), NFSC (21321001) the Key Research Program of the Chinese Academy of Sciences (KGZD-EW-201-1).

Notes and references

1 L. Kronik and A. Tkatchenko, *Acc. Chem. Res.*, 2014, **47**, 3208; Z. Zhang and M. J. Zaworotko, *Chem. Soc. Rev.*, 2014, **43**, 5444; T. S. Thakur, R. Dubey and G. R. Desiraju, *Annu. Rev. Phys. Chem.*, 2015, **66**, 21.
2 O. M. Yaghi, M. O'Keeffe, N. W. Ockwig, H. K. Chae, M. Eddaoudi and J. Kim, *Nature*, 2003, **423**, 705; B. Moulton and M. J. Zaworotko, *Chem. Rev.*, 2001, **101**, 1629; W. K. Burton, N. Cabrera and F. C. Frank, *Philos. Trans. R. Soc. London, Ser. A*, 1951, **243**, 299.
3 H. Weihe and H. U. Gudel, *Comments Inorg. Chem.*, 2000, **22**, 75; S. Ohkoshi, T. Iyoda, A. Fujishima and K. Hashimoto, *Phys Rev B*, 1997, **56**, 11642.
4 M. Ohba and H. Okawa, *Coord. Chem. Rev.*, 2000, **198**, 313.
5 F. Pan, Z. M. Wang and S. Gao, *Inorg. Chem.*, 2007, **46**, 10221.
6 R. Lescouezec, L. M. Toma, J. Vaissermann, M. Verdaguer, F. S. Delgado, C. Ruiz-Perez, F. Lloret and M. Julve, *Coord. Chem. Rev.*, 2005, **249**, 2691; J. Y. Yang, M. P. Shores, J. J. Sokol and J. R. Long, *Inorg. Chem.*, 2003, **42**, 1403.
7 D. Shao, S.-L. Zhang, X.-H. Zhao and X.-Y. Wang, *Chem. Commun.*, 2015; S. Hayami, Z. Gu, Y. Einaga, Y. Kobayasi, Y. Ishikawa, Y. Yamada, A. Fujishima and O. Sato, *Inorg. Chem.*, 2001, **40**, 3240.
8 E. J. O'Neil and B. D. Smith, *Coord. Chem. Rev.*, 2006, **250**, 3068; K. H. Choi and A. D. Hamilton, *J. Am. Chem. Soc.*, 2001, **123**, 2456; K. Araki, K. Inada and S. Shinkai, *Angew. Chem. Int. Ed. Engl.*, 1996, **35**, 72.
9 S. M. Nelson, *Pure Appl. Chem.*, 1980, **52**, 2461; M. G. B. Drew, A. H. B. Othman, S. G. McFall, P. D. A. McIlroy and S. M. Nelson, *J. Chem. Soc. Dalton Trans.*, 1977, **12**, 1173.
10 A. H. Othman and S. W. Ng, Acta Crystallogr. Sect. C: Cryst. Struct. Commun., 1995, **51**, 1059.
11 J. R. Li, R. J. Kuppler and H. C. Zhou, *Chem. Soc. Rev.*, 2009, **38**, 1477.
12 G. Wu, J. Bai, Y. Jiang, G. Li, J. Huang, Y. Li, C. E. Anson, A. K. Powell and S. Qiu, *J. Am. Chem. Soc.*, 2013, **135**, 18276.
13 Q. Zhang, A. Geng, H. Zhang, F. Hu, Z. H. Lu, D. Sun, X. Wei and C. Ma, *Chem-Eur J*, 2014, **20**, 4885.

14 S. K. Sahu, D. K. Unruh, T. Z. Forbes and A. Navrotsky, *Chem. Mater.*, 2014, **26**, 5105; C. R. Murdock and D. M. Jenkins, *J. Am. Chem. Soc.*, 2014, **136**, 10983; F. Chang, Z. M. Wang, H. L. Sun, S. Gao, G. H. Wen and X. X. Zhang, *Dalton Trans.*, 2005, **18**, 2976.
15 O. Kahn, Comments on Condensed Matter Physics, 1994, **17**, 39.
16 S. Gómez-Coca, A. Urtizberea, E. Cremades, P. J. Alonso, A. Camón, E. Ruiz and F. Luis, *Nat Commun*, 2014, **5**.
17 R. Jeffrey, *Chem. Commun.*, 2012, **48**, 3927; P. P. Samuel, K. C. Mondal, N. Amin Sk, H. W. Roesky, E. Carl, R. Neufeld, D. Stalke, S. Demeshko, F. Meyer and L. Ungur, *J. Am. Chem. Soc.*, 2014, **136**, 11964; J. M. Zadrozny, M. Atanasov, A. M. Bryan, C.-Y. Lin, B. D. Rekken, P. P. Power, F. Neese and J. R. Long, *Chemical Science*, 2013, **4**, 125.
18 X.-C. Huang, C. Zhou, D. Shao and X.-Y. Wang, *Inorg. Chem.*, 2014, **53**, 12671.

1 **Scheme 1**: Synthesis of CoL_{N3O2} precursor.

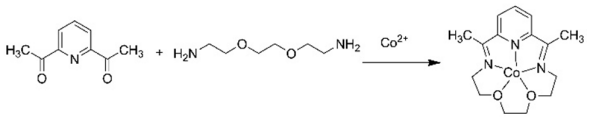

2

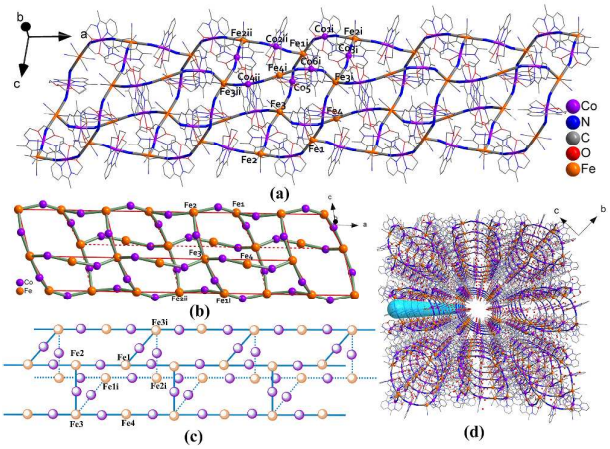

Figure1: Structural demonstration of 1. a) Tubular skeleton, non-skeleton organic atoms are dimmed; b) Connection and topology schematic diagram, grey bonds representing cyanide connections, redlines drawing the topo framework. c) Schematic diagram for demonstrating the ladder substructures. d) The packing diagram facing a direction. (Symmetry operations: i: 1-x, 2-y, 1-z; ii: –x, 2-y, 1-z)

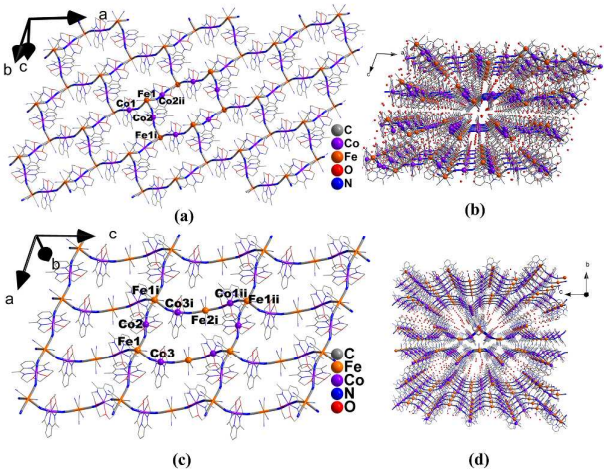

Figure 2: a) Planar structure of **2** (symmetry operations: i: 0.5-x,0.5+y,0.5-z; ii: 0.5-x, -0.5+y, 0.5-z), c) Planar structure of **3** (symmetry operations: i: -1+x,y,z; ii:-1+x,y,1+z), and their packing diagrams: b) **2** facing ***b*** direction, d) **3** facing ***a*** direction.

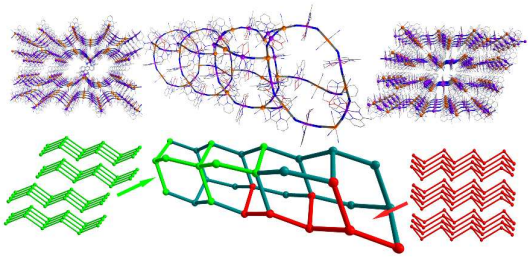

Polymorphous Fe-Co heterometallic crystals with interestingly related structures based on the same sub-structures was prepared and studied.